

# Determination of Material Properties for ANSYS Progressive Damage Analysis of Laminated Composites

Ever J. Barbero<sup>a</sup>, Mehdi Shahbazi<sup>b, c</sup>

<sup>a</sup>Corresponding author: West Virginia University, Morgantown, WV, USA

<sup>b</sup>Graduate research assistant. West Virginia University, Morgantown, WV, USA

<sup>c</sup>Final publication available at <https://doi.org/10.1016/j.compstruct.2017.05.074>

---

## Abstract

A method is presented to calculate the material parameters required by the progressive damage analysis (PDA) material-model in ANSYS®. The proposed method is based on fitting results calculated with PDA to experimental data by using Design of Experiments and Direct Optimization. The method uses experimental modulus-reduction vs. strain data for only two laminates to fit all the parameters required by PDA transverse/shear damage mode. Fitted parameters are then used to predict and compare with the experimental response of other laminates. Mesh sensitivity of PDA is studied by performing p- and h-mesh refinement. PDA can then be used to predict the response with damage evolution of any layup.

**Keywords:** ANSYS; Matrix damage; Parameter identification; Damage model; Damage parameters; In situ; Fracture.

---

## 1. Introduction

Damage initiation and propagation in composite materials are of particular importance for the design, production, certification, and monitoring of an increasingly large variety of structures. While most models are implemented on shell-type formulations, some are implemented on solid-type finite element formulations [1].

One approach is to predict the response of each lamina using a meso-model that couples the behavior of each lamina with adjacent interlaminar layers [2]. An intralaminar damage model takes into account the effects of transverse matrix crack and the interlaminar layer takes into account delaminations. Parameter identification and validation with open-hole tensile tests on quasi-isotropic laminates is described in [3].

Another approach is to use serial-parallel mixing theory [4, 5, 6], or multi-continuum theory (MCT) [7], to simulate the onset and propagation of transverse matrix cracking and other failure mechanisms. The composite response is obtained from the constitutive behavior of its constituents, each one of them simulated with its own constitutive law. In this way, it is possible to use any given non-linear material model, such as damage or plasticity, to characterize the constituents. The accuracy of damage onset and evolution predictions depends on the accuracy of the constituent models used.

Most of the models developed specifically to address the phenomenon of transverse matrix cracking are meso-models, meaning that each lamina is considered to be a homogeneous, orthotropic material [8]. Some models, such as Progressive Damage Analysis (PDA) use strength properties to predict damage onset, and fracture mechanics properties to predict damage evolution [9, 10]. Others, such as Discrete Damage Mechanics (DDM) [11] use only fracture mechanics properties to predict both damage initiation and damage evolution.

Regardless of how initiation is predicted, evolution is commonly predicted by establishing a relation between the available strain energy in the material and the density of matrix cracks [12, 13, 14, 15, 16]. For example, [17] uses Finite Fracture Mechanics (FFM) to obtain the energy release rate required to double the crack density, by propagation of a new crack between two existing cracks, or by continuous variation of crack density [18]. Similarly, the equivalent constrained model (ECM) [19, 20], defines a law that provides the evolution of stiffness as a function of matrix crack density.

Regarding the solution of the stress and strain field in the vicinity of a crack, which is necessary to calculate the strain energy release rate (ERR), most models approximate the problem as being periodic. However, numerical models such as PDA are not constrained by this assumption. While most models calculate the ERR using the equations of elasticity, with various degrees of approximation, others use Crack Opening Displacement approximations [14, 16, 21].

Some of the above mentioned formulations provide analytical expressions that can be used to obtain the mechanical response for simple geometry and load configurations. However, it is often necessary to include the constitutive model into Finite Element Analysis (FEA) software. Some models have been included in commercial FEA software [9, 10, 22]. Others are available as plugins for existing FEA software [7, 23], or as user programmable features, including UMAT, UGENS, UserMAT [24], and VUMAT [1].

ANSYS Mechanical provides progressive damage analysis (PDA) starting with release 15. Furthermore, ANSYS Workbench allows optimization of any set of variables to any user defined objective defined in a Mechanical APDL (MAPDL) model by importing the APDL script into Workbench and using Design of Experiments (DoE) and Direct Optimization (DO). Since PDA is not implemented in the graphical user interface (GUI) of ANSYS Workbench, the user must use APDL commands to define the damage initiation criterion, damage evolution law, and material parameters, as described in this manuscript.

Although elastic moduli are available for many composite material systems, the same is not true for the additional material properties required by PDA. However, laminate modulus and Poisson's ratio degradation of laminated composites as a function of applied strain are available for several material systems, for example [21, 25, 26]. This study shows how to use available data to infer the material parameters required by PDA. Specifically, the main purpose of this study is to find in situ values [27] of *transverse tensile strength*  $F_{2t}$ , *in-plane shear strength*  $F_6$ , and *energy dissipation per unit area*  $G_c$  (transverse tensile/shear mode) for the material system (composite lamina) which can be used in PDA to predict damage initiation and evolution of laminated composite structures built with the same material system but different laminate stacking sequence (LSS), geometry, loads, and boundary conditions. Experimental data from [21, 25] is used for illustration in this study.

The proposed method requires experimental data in the form of laminate extensional modulus  $E_x$  reduction (or laminate shear modulus  $G_{xy}$  reduction, or laminate Poisson's ratio  $\nu_{xy}$  reduction) vs. damage for two laminates. One laminate should have a significant component of mode I (opening) crack propagation and the other a significant component of mode II (shear) crack propagation, such as for example  $[0/90]_S$  and  $[0/\pm\theta]_S$ , respectively. Extensional modulus reduction tests are the easiest to perform but the user could use laminate shear or Poisson's ratio reduction as well.

The stated objective is achieved by minimizing the error between PDA predictions and available experimental data. Once the *input* parameters  $F_{2t}$ ,  $F_6$ ,  $G_c$  are found, the accuracy of PDA predictions is checked by comparing those predictions with experimental data for other laminates that has not been used to fit the input parameters. In fact, experimental data for only two laminates are required to fit the parameters. The input parameters are fitted using an specific mesh (one element) and type of element (SHELL 181). However, several types of elements and variable mesh refinement are customarily used for the analysis of a complex structure. Therefore, sensitivity of the PDA predictions with respect to mesh refinement and element type (quadratic vs. linear) is assessed in this work by performing both p- and h-refinement.

## 2. Progressive Damage Analysis

To perform progressive damage analysis of composite materials, the user needs to provide linear elastic orthotropic material properties and two material models: damage initiation and damage evolution law.

### 2.1. Damage Initiation Criteria

With damage initiation criteria the user can define how PDA calculates the onset (initiation) of material damage. The available initiation criteria in ANSYS are Maximum Strain, Maximum Stress, Hashin, Puck, LaRC03, and LaRC04. Besides, the user can define up to nine additional criteria as user defined initiation criteria, but only the Hashin criterion works with PDA. The remaining only work with instant stiffness reduction (MPDG). The later is similar to ply-drop off but the amount of stiffness drop can be specified in the range 0–100% of the undamaged stiffness. With MPDG, the user can choose failure criteria among those mentioned for each of the damage modes, which are assumed to be uncoupled.

Using the Hashin initiation criteria [28], PDA incorporates the following four modes of damage initiation: fiber tension, fiber compression, matrix tension, and matrix compression, which are represented by damage initiation indexes  $I_{ft}$ ,  $I_{fc}$ ,  $I_{mt}$  and  $I_{mc}$  that indicate whether a damage initiation criterion in a damage mode has been satisfied or not. Damage initiation occurs when any of the indexes exceeds 1.0.

Damage initiation indexes are unfortunately called “failure” indexes in the literature, despite the fact that, for a properly designed laminate, usually no catastrophic “failure” occurs at that point but rather only a small amount of damage appears [29, 30, 31]. The four *damage initiation* indexes are described next.

#### 2.1.1. Fiber tension ( $\sigma_{11} \geq 0$ )

Fiber tension is a misnomer sometimes used in the literature, since this mode actually represents *longitudinal tension* of the composite lamina, not the fiber. The corresponding damage initiation index is computed as follows

$$I_f^t = \left( \frac{\sigma_{11}}{F_{1t}} \right)^2 + \alpha \left( \frac{\sigma_{12}}{F_6} \right)^2 \quad (1)$$

where  $\alpha$  determines the contribution of the in-plane shear stress to this criterion.

#### 2.1.2. Fiber Compression ( $\sigma_{11} < 0$ )

The damage initiation index for *longitudinal compression* of the composite lamina is computed as follows

$$I_f^c = \left( \frac{\sigma_{11}}{F_{1c}} \right)^2 \quad (2)$$

#### 2.1.3. Matrix tension ( $\sigma_{22} \geq 0$ )

This is also misnomer, since this mode actually represents *transverse tension and in-plane shear* of the composite lamina, not the matrix. The confusion is due to the fact that this is a matrix-dominated mode, but still the criterion is applied at the meso-scale; that is at the lamina level, not at the micro-scale where the fiber and matrix would be analyzed separately. Furthermore, the parameters involved ( $F_{2t}$ ,  $F_6$ ) are those of a lamina, not of fiber and matrix separately, and the resulting index applies to the lamina, not to the matrix

$$I_m^t = \left( \frac{\sigma_{22}}{F_{2t}} \right)^2 + \left( \frac{\sigma_{12}}{F_6} \right)^2 \quad (3)$$

#### 2.1.4. Matrix compression ( $\sigma_{22} < 0$ )

The damage initiation index for *transverse compression* of the composite lamina is computed as follows

$$I_m^c = \left(\frac{\sigma_{22}}{2F_4}\right)^2 + \left[\left(\frac{F_{2c}}{2F_4}\right)^2 - 1\right] \frac{\sigma_{22}}{F_{2c}} + \left(\frac{\sigma_{12}}{F_6}\right)^2 \quad (4)$$

where  $\sigma_{ij}$  are the components of the stress tensor;  $F_{1t}$  and  $F_{1c}$  are the tensile and compressive strengths of a lamina in the longitudinal (fiber) direction;  $F_{2t}$  and  $F_{2c}$  are the tensile and compressive strengths in the transverse direction;  $F_6$  and  $F_4$  are the in-plane and intralaminar shear strengths.

In this work, to obtain the model proposed by Hashin and Rotem [28], in (1) we set  $\alpha = 0$  and in (4)  $F_4 = 1/2F_{2c}$ . Also note that in situ strength should be used for all matrix-dominated modes [32].

The APDL command for Hashin initiation criteria for all damage modes is TB, DMGI, as it is shown below:

```
! Damage detection using failure criteria
TB, DMGI, 1, 1, 4, FCRT
TBTEMP, 0
! 4 is the value for selecting Hashin criteria,
! which is here selected for all four failure modes
TBDATA, 1, 4, 4, 4, 4
```

#### 2.2. Material Strength Limits

To evaluate the damage initiation criteria, the user defines the maximum stresses or strains that a material can tolerate before damage occurs. Required inputs depend on the chosen criteria in the damage initiation part. For instance, for Hashin criteria the user needs to define in situ tensile and compression strength in 1, 2, and 3 lamina orientations (called X, Y, and Z directions in ANSYS), and the shear strength in 12, 13, and 23 lamina planes (called XY, XZ, and YZ in ANSYS).

Since fiber dominated strength values are at least one order of magnitude (10X) larger than matrix dominated strengths, matrix modes occur much earlier in the life of the structure than fiber modes. For properly designed laminates (e.g., according to the 10% rule and other industry-accepted practices [33]) fiber modes (§2.1.1, §2.1.2) do not occur until nearly the end of the life. Furthermore, transverse matrix compression (§2.1.4) does not result in progressive damage but rather leads to sudden failure according to the Mohr-Coulomb criterion [34]. Therefore, this study focuses on matrix tension and shear modes (§2.1.3), which are known to lead to substantial progressive damage [25, 21].

Initial values of in situ transverse tensile strength  $F_{2t}$ , in situ in-plane shear strength  $F_6$ , and intralaminar shear strength  $F_4$  (called XT, XY, and XZ in ANSYS) should be defined in the APDL script. The command for material strength limit is TB, FCLI, as shown below:

```
! Material Strengths
TB, FCLI, 1, 1, 6
TBTEMP, 0
! Failure Stress, Fiber Tension
TBDATA, 1, F1t
! Failure Stress, Fiber Compression
TBDATA, 2, F1c
! Toughness Stress, Matrix Tension
TBDATA, 3, F2t
```

```

! Failure Stress, Matrix Compression
TBDATA,4,F2c
! Failure Stress, XY Shear
TBDATA,7,F6
! Failure Stress, YZ Shear
TBDATA,8,F4

```

As it was previously stated, the damage initiation part of PDA requires six material parameters listed above. Two of those,  $F_{2t}$  and  $F_6$ , are in situ values. In situ values can be calculated using equations that involve the nominal strengths of the unidirectional lamina and the corresponding *critical energy release rates* (ERRs)  $G_{Ic}$ ,  $G_{IIc}$  in modes I and II [34], or the transition thickness of the material [33, §7.2.4], [35]. However, these critical ERRs and transition thicknesses are not usually available in the literature. Experimental methods to determine in situ values are not available either. By focusing on one damage mode, namely transverse tension/shear damage (§2.1.3), it is shown in this work that the material parameters required by PDA ( $F_{2t}$ ,  $F_6$ , and  $G_c$ ) can be obtained by fitting PDA model results to suitable experimental data. Thus, critical ERRs, transition thicknesses, and in situ strength values, which are not available in the literature and are very difficult to determine experimentally, can be simply obtained with the methodology proposed herein.

### 2.3. Damage Evolution

After satisfying the selected initiation criteria, further loading will degrade the material. The damage evolution law determines how the material degrades. In ANSYS, there are two options for damage evolution: instant stiffness reduction (MPDG) and continuum damage mechanics (PDA). Since instant stiffness reduction, which is suddenly applied when the criterion is satisfied, does not provide any information about damage evolution, this study uses the PDA method for damage evolution.

PDA damage evolution requires eight parameters: four values of energy dissipated per unit area ( $G_c$ , Figure 1) and four viscosity damping coefficients ( $\eta$ ) for tension and compression in both fiber and matrix dominated modes. The energy dissipated per unit area is defined as:

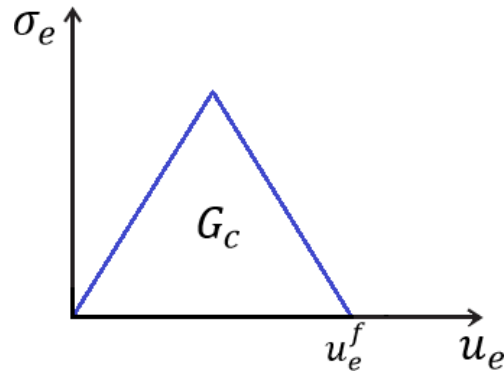


Figure 1: Equivalent stress  $\sigma_e$  vs. equivalent displacement  $u_e$ .

$$G = \int_0^{u_e^f} \sigma_e du_e \quad (5)$$

where:

$\sigma_e$  = is the equivalent stress. For simple uniaxial stress state, the equivalent stress is the actual stress. For complex stress state, the equivalent stresses and strains are calculated based on Hashin's damage initiation criteria.

$u_e$  = is the equivalent displacement. For simple uniaxial state of stress and strain,  $u_e = \epsilon_e L_c$ , with  $\epsilon_e$  is the uniaxial strain and  $L_c$  is the length of the element in the stress direction. For complex states of strain,  $\epsilon_e$  is the equivalent strain and  $L_c$  is the characteristic length of the element.

$u_e^u$  = is the ultimate equivalent displacement, where total material stiffness is lost for the specific mode.

$L_c$  is the characteristic length. For 2D elements (PLANE and SHELL), it is internally defined in terms of the area  $A_e$  of the element, as follows [36]:

$$\begin{aligned} L_c &= 1.12 \sqrt{A_e} ; \text{ for square elements} \\ L_c &= 1.52 \sqrt{A_e} ; \text{ for triangular elements} \end{aligned} \quad (6)$$

Viscous damping coefficients  $\eta$  are also specified respectively for each of the damage modes. For a specific damage mode, the damage evolution is internally regularized as follows:

$$d'_{t+\Delta t} = \frac{\eta}{\eta + \Delta t} d'_t + \frac{\Delta t}{\eta + \Delta t} d_{t+\Delta t} \quad (7)$$

where:

$d'_{t+\Delta t}$  = Regularized damage variable at current time.

$d_{t+\Delta t}$  is used for material degradation

$d'_t$  = Regularized damage variable at previous time.

$d_{t+\Delta t}$  = Un-regularized current damage variable

The damping coefficients may need to be adjusted if convergence problems are encountered, but all the cases in this work executed flawlessly by just using the default values that are built into ANSYS.

The command for defining damage evolution in APDL is TB,DMGE, as shown below.

```
! Damage Evolution with CDM Method
TB,DMGE,1,1,8,CDM
TBTEMP,0
! Fracture Toughness, Fiber Tensile
TBDATA,1,Gft
! Viscosity Damping Coefficient, Fiber Tensile
TBDATA,2,  $\eta^{ft}$ 
! Fracture Toughness, Fiber Compressive
TBDATA,3,Gfc1E6
! Viscosity Damping Coefficient, Fiber Compressive
TBDATA,4,  $\eta^{fc}$ 
! Fracture Toughness, Matrix Tensile
TBDATA,5,Gc
! Viscosity Damping Coefficient, Matrix Tensile
TBDATA,6,  $\eta^{mt}$ 
! Fracture Toughness, Matrix Compressive
```

```
TBDATA,7,Gcmc
! Viscosity Damping Coefficient, Matrix Compressive
TBDATA,8, ηmc
```

### 3. Methodology

In this section we propose a methodology using Design of Experiments (DoE) and Design Optimization (DO) to adjust the values of  $F_{2t}$ ,  $F_6$ , and  $G_c$ , so that the PDA prediction closely approximates the experimental data.

First we use DoE to identify the laminates that are most sensitive to each parameter. The focus at this point is to identify the minimum number of experiments that are needed to adjust the parameters. In this way, additional experiments conducted with different laminate stacking sequences (LSS) are not used to adjust parameters but to assess the quality of the predictions.

In principle, the DoE technique is used to find the location of sampling points in a way that the space of random input parameters  $X = \{F_{2t}, F_6, G_c\}$  is explored in the most efficient way and that the output function  $D$  can be obtained with the minimum number of sampling points. In this study the output function (also called objective function) is the error between the predictions and the experimental data. Given  $N$  experimental values of laminate modulus  $E(\epsilon_i)$ , the error is defined as

$$D = \frac{1}{N} \sqrt{\sum_{i=1}^N \left( \frac{E}{\bar{E}} \Big|_{\epsilon=\epsilon_i}^{ANSYS-PDA} - \frac{E}{\bar{E}} \Big|_{\epsilon=\epsilon_i}^{Experimental} \right)^2} \quad (8)$$

where  $\epsilon$  is the strain applied to the laminate, and  $i = 1 \dots N$ . Furthermore,  $E$  and  $\bar{E}$  are laminate elastic modulus for damaged and undamaged laminate, respectively, and  $N$  is the number of experimental data points available.

DoE tools can be found in ANSYS Workbench in the Design Explorer (DE) module, which includes also Direct Optimization (DO), Parameters Correlation, Response Surface (RS), Response Surface Optimization (RSO), and Six Sigma Analysis.

Let's denote the input parameters by the array  $X = \{F_{2t}, F_6, G_c\}$ . In this case, the output function  $D = D(X)$  can be calculated by evaluation of eq. (8) through execution of the finite element analysis (FEA) code for  $N$  values of strain. Each FEA analysis is controlled by the APDL script, which calls for the evaluation of the non-linear response of the damaging laminate for each value of strain, with parameters  $X$ . If the mesh is refined, these evaluations could be computationally intensive.

An alternative to direct evaluation of the output function is to approximate it with a multivariate quadratic polynomial. The approximation is called response surface (RS). It can be constructed with only few actual evaluations of the output by choosing a small number of sampling points for the input. The sampling points are chosen using Design of Experiments (DoE) theory. The number of evaluations needed to construct the response surface (RS) and for direct optimization (DO) are shown in Table 1.

The shape of the response surface can be inferred by observing the variation of the output  $D$  as a function of one input at a time. This is shown in Figures 2, 3, and 4, for laminate #1 (Table 2). The abscissa spans each of the inputs and the ordinate measures the error (8) between predicted and experimental data.

By observing the RS we can understand which parameters (inputs) have most effect on the error (output). From Figure 4 it is clear that the error is not sensitive to  $F_6$  for laminate #1. This is because no lamina in laminate #1 is subject to shear. Therefore, it is decided to use the experimental data of laminate #1 to evaluate

Table 1: Number of FEA evaluations used (a) to construct the response surface (RS) and (b) to adjust the input parameters by direct optimization (DO).

| # of inputs | Inputs             | # of evaluations |                |
|-------------|--------------------|------------------|----------------|
|             |                    | RS               | DO (screening) |
| 1           | $F_6$              | 5                | 100            |
| 2           | $F_6, G_c$         | 9                | 100            |
| 3           | $F_{2t}, F_6, G_c$ | 15               | 100            |

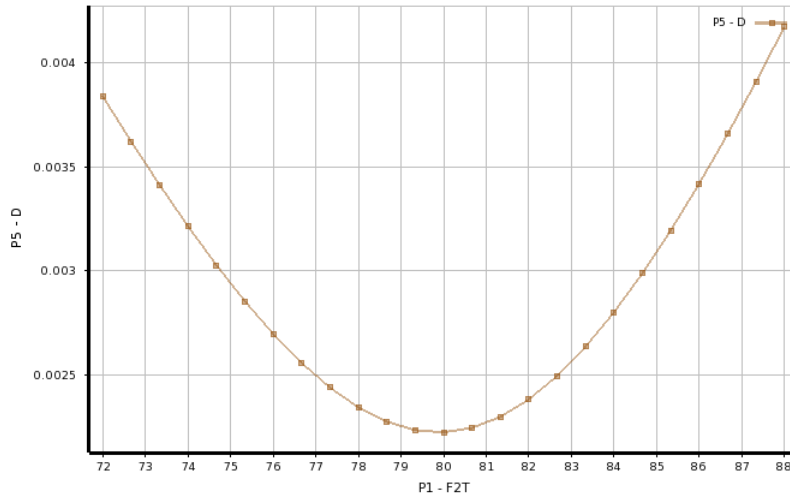


Figure 2: Response surface chart. Error (D) vs.  $F_{2t}$ .

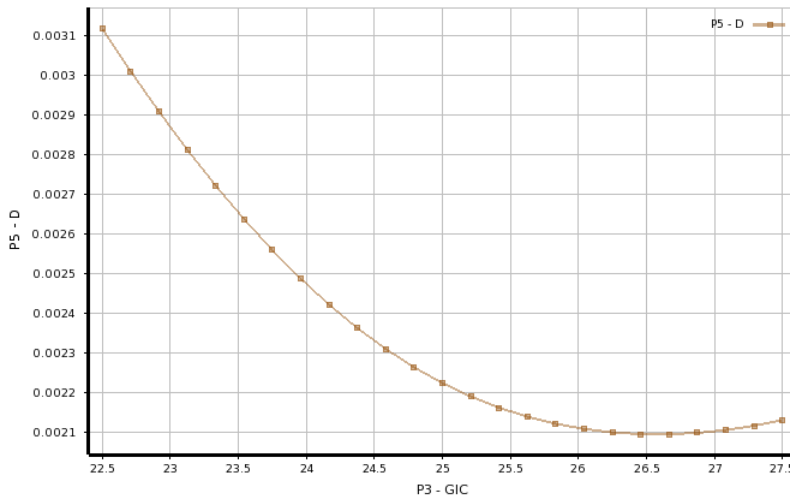


Figure 3: Response surface chart. Error (D) vs.  $G_c$ .



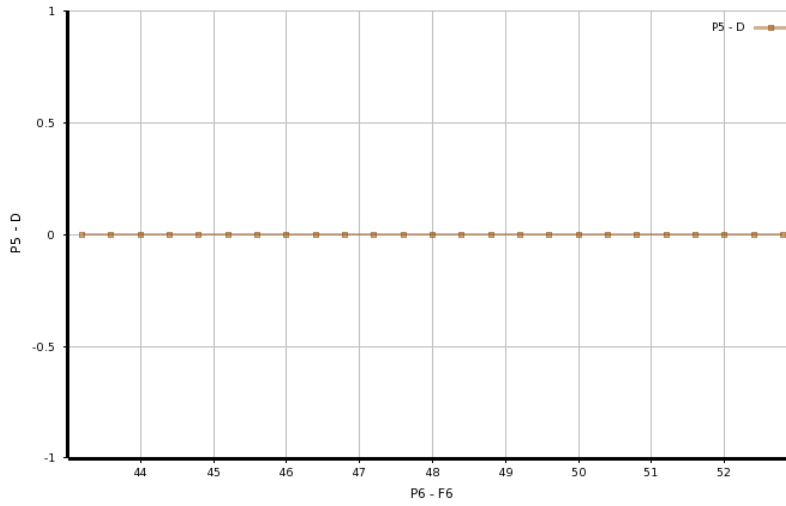


Figure 4: Response surface chart. Error (D) vs.  $F_6$ .

Table 2: Laminate stacking sequence for all laminates for which experimental data is available [21, 25].

| Laminate # | LSS                      |
|------------|--------------------------|
| 1          | $[0_2/90_4]_S$           |
| 2          | $[\pm 15/90_4]_S$        |
| 3          | $[\pm 30/90_4]_S$        |
| 4          | $[\pm 40/90_4]_S$        |
| 5          | $[0/90_8/0_{1/2}]_S$     |
| 6          | $[0/\pm 70_4/0_{1/2}]_S$ |
| 7          | $[0/\pm 55_4/0_{1/2}]_S$ |
| 8          | $[0/\pm 40_4/0_{1/2}]_S$ |
| 9          | $[0/\pm 25_4/0_{1/2}]_S$ |

Table 3: Sensitivity  $S$  of the output (error) to each input (parameter).

| Input    | Input range |      | Error D    |            |            | Sensitivity | Laminate |
|----------|-------------|------|------------|------------|------------|-------------|----------|
|          | min         | max  | min( $D$ ) | max( $D$ ) | ave( $D$ ) | $S$         | #        |
| $F_{2t}$ | 72          | 88   | 0.0022     | 0.0041     | 0.00297    | 0.64        | #1       |
| $G_c$    | 22.5        | 27.5 | 0.0031     | 0.0020     | 0.0026     | -0.42       | #8       |
| $F_6$    | 50          | 88   | 0.076      | 0.102      | 0.093      | -0.28       | #8       |

only two input parameters ( $F_{2t}$  and  $G_c$ ). This makes the optimization algorithm to run faster. The charts in Figures 2–4 are drawn for the input ranges given in Table 3.

The RS is a multivariate quadratic polynomial that approximates the actual output function  $D(X)$  as a function of the input variables. In this study,  $D_{RS} = f(X_i)$ . The sensitivity  $S$  of the output to input  $X$  in the user specified interval  $[X_{min}, X_{max}]$  is calculated as

$$S = \frac{\max(D) - \min(D)}{\text{average}(D)} \quad (9)$$

and tabulated in Table 3. Note that the sensitivity can be calculated from the error evaluated directly from FEA analysis (DO) or from Response Surface (RS). The later is much more expedient than the former, as it can be seen in Table 1, considering the number of evaluations needed.

The input parameters can be adjusted with any mesh and any type of elements that represent the gage section of the specimen, or a single element to represent a single material point of the specimen. For expediency, a single linear element (SHELL 181) is used in this study.

### 3.1. APDL

ANSYS Parametric Design Language (APDL) [24] must be used in order to predict damage with PDA [36]. In this study, we need three *input* parameters:  $F_{2t}$ ,  $F_6$ ,  $G_c$  and one *output* parameter:  $D$ . In APDL, *parameters* are defined dynamically, just by giving them a name and value, as follows:

```
/TITLE, Laminate #1: [0-2/90-4]s
/UNITS,MPA                ! Units are in mm, MPa, and Newtons
/PREP7
F2t = 80.0                 ! MPa
F6 = 48.0                  ! MPa
Gc = 25.0                  ! kJ/m^2
```

Next, APDL commands are used to specify the element type, the laminate stacking sequence (LSS) with SECDATA command (Table 2), the elastic properties with MP command (Table 4), and the material strengths with TB command (Table 4). The material strengths values given above for  $F_{2t}$ ,  $F_6$ , are simply initial (guess) values for the optimization.

```
ET,1,SHELL181             ! Element type
! LAMINATE STACKING SEQUENCE
SECTYPE,1,SHELL,,#1      ! SECTYPE, SEID, TYPE, SUBTYPE, NAME
SECDATA,0.288,1,0        ! thickness, material, angle
SECDATA,1.152,1,90
SECDATA,0.288,1,0
! ORTHOTROPIC MATERIAL PROPERTIES
```

```

MP,EX,1,44.7E3
MP,EY,1,12.7E3
MP,EZ,1,12.7E3
MP,GXY,1,5.8E3
MP,GYZ,1,4.5E3
MP,GXZ,1,5.8E3
MP,PRXY,1,0.297
MP,PRYZ,1,0.4111
MP,PRXZ,1,0.297
! STRENGTH VALUES
TB,FCLI,1,1,6          ! material strengths
TBTEMP,0
TBDATA,1,1020         ![F1t]  FIBER TENSION
TBDATA,2,-620         ![F1c]  FIBER COMPRESSION
TBDATA,3,F2t          ![F2t]  MATRIX TENSION (guess value)
TBDATA,4,-140         ![F2c]  MATRIX COMPRESSION
TBDATA,7,F6           ![F6]   FAILURE STRESS, XY SHEAR (guess)
TBDATA,8,52.7         ![F4]   FAILURE STRESS, YZ SHEAR

```

Also the APDL script contains values for the eight damage evolution parameters with TBDDATA command (Table 5). The strengths of the non-participating modes (FT,FC, and MC) are set to a high value to avoid those modes from interfering with the study of the MT mode, and the values of the corresponding damping coefficients  $\eta$  are thus irrelevant. The energy dissipation per unit area to be adjusted ( $G_c$ ) is set to a guess value, and the corresponding damping coefficient is found by trial and error to obtain a smooth computation of the entire plot of laminate modulus vs. applied strain, as it can be seen in Figure 5.

```

!DAMAGE initiation (DMGI)
TB,DMGI,1,1,4,FCRT    ! Damage detection using failure criteria
TBTEMP,0
TBDDATA,1,4,4,4,4     ! Hashin criteria for all 4 failure modes
!DAMAGE EVOLUTION (DMGE)
TB,DMGE,1,1,8,CDM     ! damage evolution with CDM method
TBTEMP,0
TBDDATA,1,1E6         ! Fracture toughness, fiber tensile
TBDDATA,2,0.001       ! damping coefficient, fiber tensile
TBDDATA,3,1E6         ! dissipation energy, fiber compressive
TBDDATA,4, 0.001     ! damping coefficient, fiber compressive
TBDDATA,5,Gc          ! dissipation energy, matrix tensile
TBDDATA,6, 0.005     ! damping coefficient, matrix tensile
TBDDATA,7,1E6         ! dissipation energy, matrix compressive
TBDDATA,8, 0.001     ! damping coefficient, matrix compressive

```

The APDL script is also used to specify the mesh, boundary conditions, and loading. At this point, the analyst can enter mesh, boundary conditions, and loading for whatever structure he/she wishes to analyze. In this work, the strain applied to the laminate is specified by imposing a specified displacement. Incrementation of the applied displacement is implemented to mimic the experimental data, which is available for a finite set of values of applied strain.

```

! GEOMETRY AND LOAD
RECTNG,0,55,0,10      ! Creates rectangle with x=55 m and y=1 m
ESIZE,55              ! Element size 100 mm

```

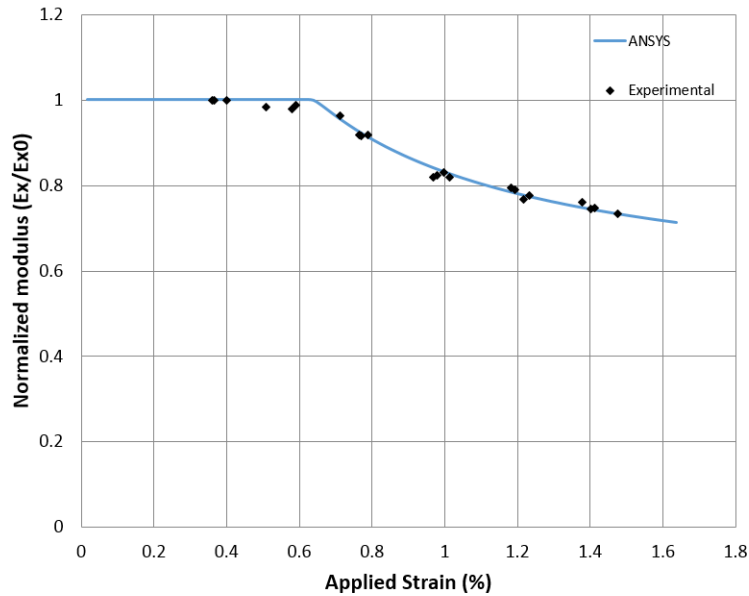


Figure 5: Normalized modulus vs. applied strain for laminate  $[0_2/90_4]_s$ .

```

AMESH,all           ! Mesh the area
FINISH              ! Exit pre-processor module
! LOADING AND BC
/SOLU               ! Start Solution module
ANTYPE,STATIC
OUTRES,ALL,1       ! Store results for each substep
D,1,all             ! Define b.c. on node 1, totally fixed
D,2,ROTX,0.00
D,2,ROTZ,0.00
D,2,UY,0.00
D,2,UX,.9           ! Define b.c. on node 2, Uy=0.0
D,3,UX,.9           ! Define displacement on node 3, Ux=0.1
D,4,UX,0.00
D,4,ROTY,0.0
D,4,ROTZ,0.0       ! Define b.c. on node 4, Ux=0.0
NSUBST,100,200,100 ! 100 = Number of substeps this load step
SOLVE              ! Solve load step
FINISH             ! Exit solution module

```

The APDL script also includes a table with experimental data for the laminate being analyzed. Such data consists of a number  $N$  of pairs of values representing laminate modulus as a function of applied strain  $E_x(\epsilon_x)$ .

```

! RESULTS
NDATA=22
*DIM,AA,ARRAY,NDATA,2,1, , ,
*SET,AA(1,1,1) , 0.35909

```

```
*SET,AA(1,2,1) , 1
...
*SET,AA(22,1,1) , 1.47645
*SET,AA(22,2,1) , 0.733498
```

Finally, the APDL script calculates the error as per eq. (8). For each data point, the script loops over the solution points to find the point with strain closest to the data point.

```
/POST26          ! Start time-history post-processing
NSOL,2,3,U,X, UXnode3 ! Load displacements node 3
RFORCE,3,4,F,X,FXnode4 ! Load reaction force node 4
RFORCE,4,1,F,X,FXnode1 ! Load reaction force node 1
LINES,1000
PRVAR,2,3,4      ! list displacements and reactions
VGET,UX3,2,0
VGET,FX4,3,0
VGET,FX1,4,0
L=0
*DO,I,1,NDATA,1
*DO,J,1,100,1
SXP=AA(I,1,1)
EEXP=AA(I,2,1)
SCS=1.8181*UX3(J,1)
FN4=FX4(J,1)
FN1=FX1(J,1)
FN2=FX1(2,1)
SCS2=1.8181*UX3(2,1)
MRG=ABS((SCS-SXP))
*IF,MRG,LE,0.008145,THEN
NUM=((FN1+FN4)*(SCS2))
DEN=2*(FN2)*(SCS)
EPE=NUM/DEN
ER1=EPE-EEXP
ER2=ER1*ER1
L=L+ER2
*ENDIF
*ENDDO
*ENDDO
D=(1/NDATA)*SQRT(L)
FINISH          ! Exit post-processing module
```

### 3.2. Workbench

The APDL script is able to compute the error  $D$  for a given set of *input* material parameters. The actual material parameters are now found by minimizing the error using Design Optimization (DO), which is available in Workbench [37]. For this, a *Mechanical APDL* component is added to the Project Schematic of Workbench by dragging it from the Component Systems menu. The APDL code is then imported into Workbench, as shown in Figure 6.

Table 4: Lamina elastic properties and in situ strength values.

| Property      | Units | Value | Ref.        |
|---------------|-------|-------|-------------|
| $E_1$         | MPa   | 44700 | [25]        |
| $E_2$         | MPa   | 12700 | [25]        |
| $G_{12}$      | MPa   | 5800  | [25]        |
| $\nu_{12}$    | -     | 0.297 | [25]        |
| $\nu_{23}$    | -     | 0.411 | [25]        |
| Ply thickness | mm    | 0.144 | [21]        |
| $F_{1t}$      | MPa   | 1020  | [33]        |
| $F_{1c}$      | MPa   | -620  | [33]        |
| $F_{2t}$      | MPa   | 80    | guess value |
| $F_{2c}$      | MPa   | -140  | [33]        |
| $F_6$         | MPa   | 48    | guess value |
| $F_4$         | MPa   | 52.7  | [33]        |

Table 5: Damage evolution parameters for the lamina.

| Property      | Units             | Value | Ref.            |
|---------------|-------------------|-------|-----------------|
| $G_f^{ft}$    | KJ/m <sup>2</sup> | 1E6   | high value      |
| $G_f^{fc}$    | KJ/m <sup>2</sup> | 1E6   | high value      |
| $G_c$         | KJ/m <sup>2</sup> | 25    | guess value     |
| $G_m^{mc}$    | KJ/m <sup>2</sup> | 1E6   | high value      |
| $\eta_f^{ft}$ | -                 | 1E-3  | immaterial      |
| $\eta_f^{fc}$ | -                 | 1E-3  | immaterial      |
| $\eta_m^{mt}$ | -                 | 5E-3  | trial and error |
| $\eta_m^{mc}$ | -                 | 1E-3  | immaterial      |

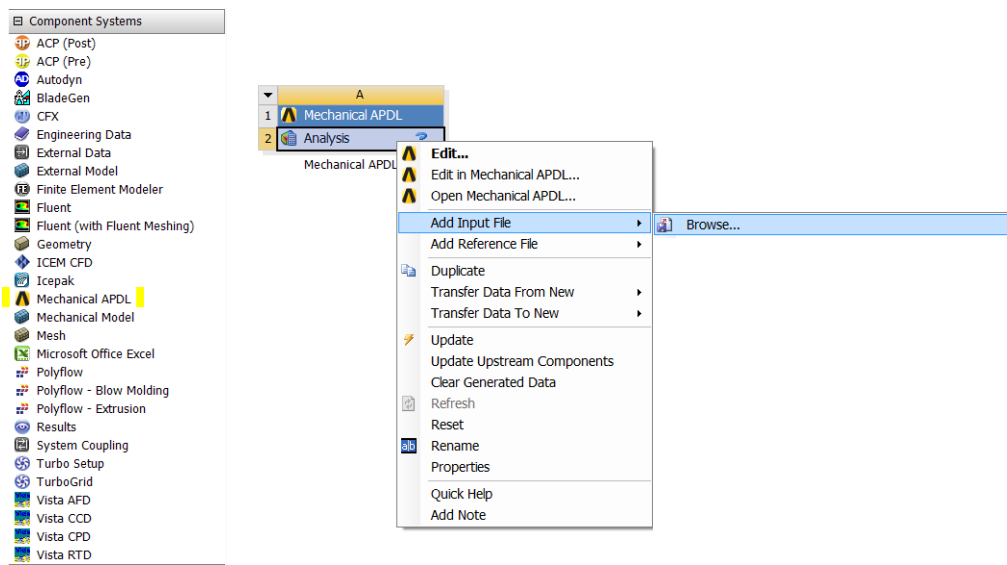


Figure 6: Importing the APDL code into Workbench.

Next, from among all the parameters defined in the APDL script, the input parameter ( $F_{2t}$ ,  $F_6$ ,  $G_c$ ) and output parameters ( $D$ ) are selected as shown in Figure 7.

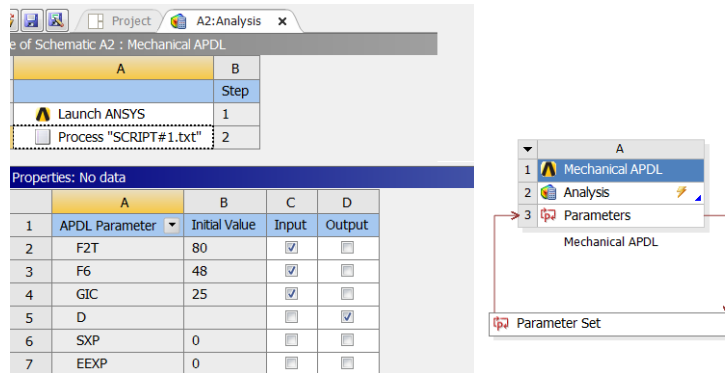


Figure 7: Inputs and output parameters are selected.

### 3.3. Optimization

Optimization techniques are used in this study to minimize the error (8) by adjusting the input (material) parameters ( $F_{2t}$ ,  $F_6$ ,  $G_c$ ). In these way, the final values of these parameters represent the damaging behavior of the material system as described by the specific PDA material model used in the underlying FEA.

A *Response Surface Optimization (RSO)* component is now added to Workbench by dragging it from the Component Systems menu to the Project Schematic (Figure 8).

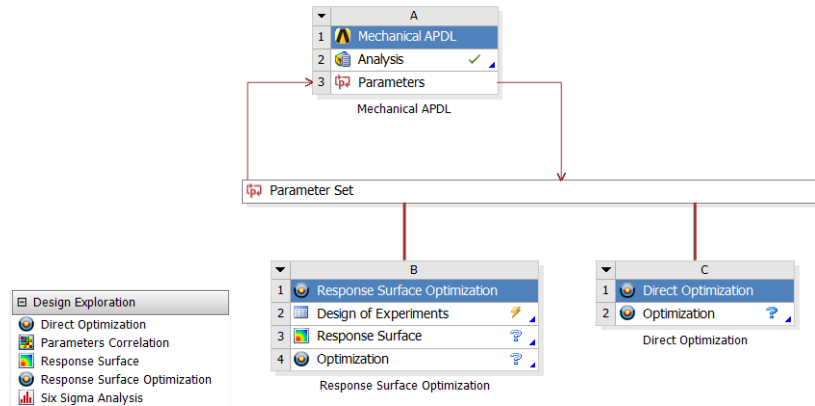


Figure 8: Response Surface tools include DoE, RS, and RS Optimization.

Then, DoE is used to adjust a multivariate quadratic polynomial to the actual response (output) of the system as defined by the APDL script. The multivariate are the input parameters, which in this study are three parameters.

Then, the RS is used to plot the response (output) vs. each of the input parameters and to calculate the sensitivities. This allows the user to select, for optimization, only the parameters to which the output



Table 6: Error and adjusted values of input (material) parameters for all laminates considered; “–” means that for those laminates, the parameters are those adjusted with the other two laminates, and “insensitive” means that that property has no effect on the response for that laminate.

| Laminate | Error $D$ |          | Adjusted values |       |             |
|----------|-----------|----------|-----------------|-------|-------------|
|          | RS        | DO       | $F_{2t}$        | $F_6$ | $G_c$       |
| #1       | 0.002046  | 0.002007 | 78.32           | 86.70 | insensitive |
| #2       | 0.003063  | 0.002682 | –               | –     | insensitive |
| #3       | 0.010447  | 0.007820 | –               | –     | insensitive |
| #4       | 0.011243  | 0.006047 | –               | –     | insensitive |
| #5       | 0.015960  | 0.015278 | –               | –     | –           |
| #6       | 0.011002  | 0.010491 | –               | –     | –           |
| #7       | 0.052601  | 0.051115 | –               | –     | –           |
| #8       | 0.076554  | 0.075605 | –               | –     | 26.98       |
| #9       | 0.022765  | 0.020154 | –               | –     | –           |

Table 7: Comparison of adjusted input (material) parameters obtained by using Response Surface (RS) and Direct Optimization (DO) Screening and Adaptive Single Objective.

| Parameter                | Optimization method |                 |                 |
|--------------------------|---------------------|-----------------|-----------------|
|                          | RSO                 | DO <sup>a</sup> | DO <sup>b</sup> |
| $F_{2t}$                 | 80.01               | 78.32           | 78.55           |
| $F_6$                    | 87.13               | 86.70           | 88.00           |
| $G_c$                    | 26.72               | 26.98           | 27.50           |
| Max # of FEM evaluations | 15                  | 100             | 33              |

<sup>a</sup> Screening, <sup>b</sup> Adaptive Single-Objective.

(error) is sensitive. This minimizes the need for experimentation to only two laminate stacking sequences (samples), but these two samples must be chosen judiciously so that they provide maximum sensitivity of the *output* (error) to the *input* parameters. Through this process, laminates #1 and #8 were selected.

Within RSO, optimization is performed by using the RS rather than actual evaluation of the response via finite element analysis (FEA). This results in significant savings of computer time, but the result is approximate because the RS is an approximation to the actual output function.

To get exact optimum parameters (within numerical accuracy) one has to conduct Direct Optimization (DO). It can be seen in Table 6 that RS is quite accurate when compared with DO, considering that the number of FEA evaluations is smaller for RS than for DO. As it is shown in Table 7, the accuracy of the parameters is good when RSO is used instead of DO. However, it must be noted that for a one-element mesh the computational cost is insignificant. The two alternatives are noted in case calibration were to be attempted modeling a complex test setup (such cruciform, tube, Iosipescu, etc.) where the computational cost may be an issue.

Twenty-two experimental data points are available for laminate #1 and nineteen experimental data points are available for laminate #8. Laminate #1 ( $[0_2/90_4]_S$ ) was chosen because this laminate is sensitive to  $F_{2t}$  and  $G_c$ . On the contrary,  $F_6$  does not have any effect on the results of Laminate #1, as shown in Table 3 and Fig. 9. It can be seen that the response of laminate #1 is insensitive to  $F_6$ . Furthermore, only values of  $F_{2t}$  and  $G_c$  (not  $F_6$ ) are sufficient to accurately predict the behavior of laminate #1, as shown in Figure 5.

For minimizing the error  $D$ , lower and upper limits must be chosen for each input, as shown in Table 3. Three candidate design points are then found in that range, as shown in Fig. 10. Since the response surface

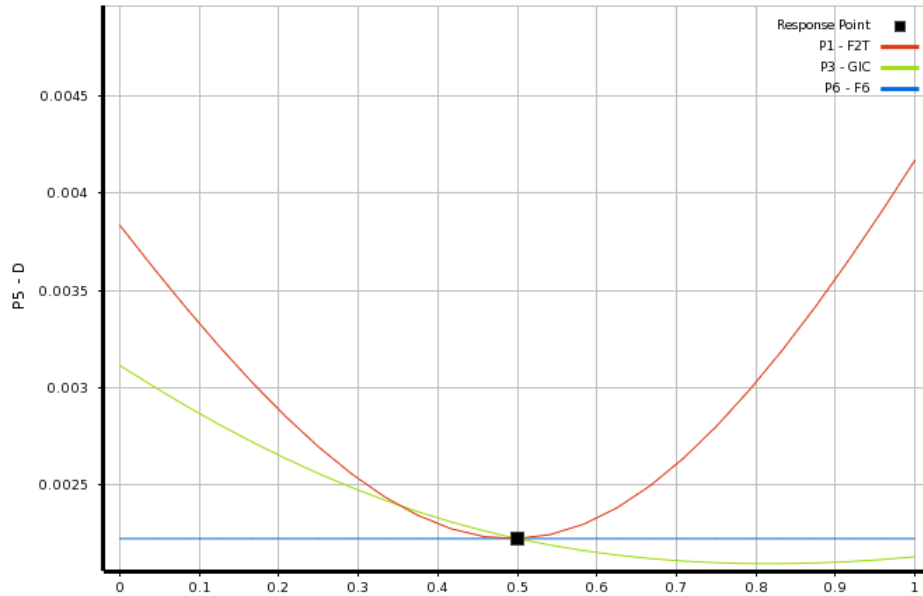


Figure 9: Sensitivity of error  $D$  (ordinate) to inputs  $F_{2t}$ ,  $G_c$ , and  $F_6$  (abscissa) for laminate #1. Inputs ranges are mapped to the interval  $[0-1]$  along the abscissa to show all three curves in the same figure.

is approximate (performing actual evaluation via FEA for only a few points), direct optimization is used to check for accuracy. Direct optimization performs FEA for all the points explored by the optimization algorithm. Results from response surface (RS) and direct optimization (DO) are compared in Table 7.

Since values of  $F_{2t}$  and  $G_c$  are found with laminate #1, the only parameter that remains to be found is  $F_6$ . For this purpose, laminate #8 ( $[0/\pm 40/0_{1/2}]_S$ ) is chosen because it experiences shear stress in the  $\pm 40^\circ$  laminas. In this way,  $F_6$  has a visible effect on the error ( $D$ ), as shown in Fig. 11.

#### 4. Comparison with experiments

In this section, predicted laminate modulus  $E_x(\epsilon_x)$  with parameters listed in Table 7 are compared with experimental data for all the laminates. The error (8) for each laminate is reported in Table 6.

Laminates #1 through 5 have a cluster of 8 plies in the layer that is subject to transverse matrix cracking (Table 2). Since the in situ transverse tensile strength was adjusted with laminate #1, damage onset can be predicted well with PDA, as shown in Figures 5, and 12 through 14, but not on laminates #6 through #9 (Figures 17–18) because in those the cracking cluster has only 4 plies (Table 2). Recall that the in situ strength varies with the thickness of the cracking cluster [33, §7.2.4].

To accurately predict damage initiation, the PDA parameters  $F_{2t}$ ,  $F_6$ , must be in situ values. But in situ values are inversely proportional to the square root of cluster thickness [33, §7.2.4]. The PDA implementation in ANSYS does not allow for correction of in situ values as a function of cluster thickness. Software implementation of such correction is possible [38] but cumbersome as one has to identify clusters, and surface clusters behave as having double their actual thickness [33, §7.2.4]. In summary, the in situ strength values  $F_{2t}$  and  $F_6$  should be adjusted with data from laminates with cluster thickness expected in practice. This is not always feasible, given the variety of laminates usually employed in design.

| Table of Schematic C4: Optimization |                     |   |                   |                   |
|-------------------------------------|---------------------|---|-------------------|-------------------|
|                                     | A                   | B   | C                 | D                 |
| 1                                   | Optimization Study  |   |                   |                   |
| 2                                   | Minimize P5         | Goal, Minimize P5 (Default importance)  |                   |                   |
| 3                                   | Optimization Method |   |                   |                   |
| 4                                   | Screening           | The Screening optimization method uses a simple approach based on sampling and sorting. It supports multiple objectives and constraints as well as all types of input parameters. Usually it is used for preliminary design, which may lead you to apply other methods for more refined optimization results. |                   |                   |
| 5                                   | Configuration       | Generate 1000 samples and find 3 candidates.  |                   |                   |
| 6                                   | Status              | Converged after 1000 evaluations.   |                   |                   |
| 7                                   | Candidate Points    |   |                   |                   |
| 8                                   |                     | Candidate Point 1   | Candidate Point 2 | Candidate Point 3 |
| 9                                   | P1 - F2T            | 80.011  | 79.096            | 78.136            |
| 10                                  | P3 - GIC            | 26.723  | 26.829            | 27.473            |
| 11                                  | P5 - D              | ★★★ 0.0019932   | ★★★ 0.0020194     | ★★★ 0.0021065     |

Figure 10: Candidate designs.

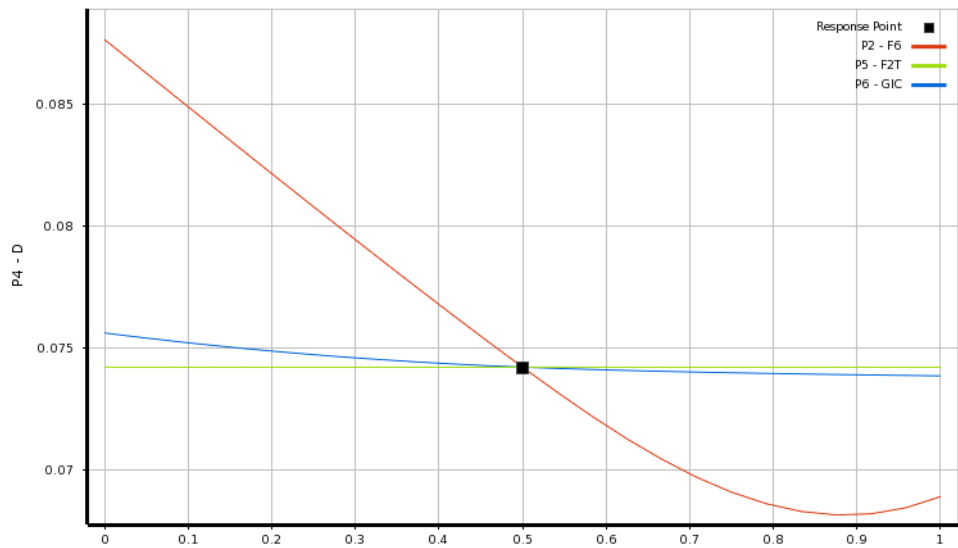


Figure 11: Sensitivity curves show how sensitive the error  $D$  (ordinate) is to inputs  $F_{2t}$ ,  $G_m^t$ , and  $F_6$  (abscissa) for laminate #8. Inputs ranges are mapped to the interval [0–1] along the abscissa to show all three curves in the same figure.

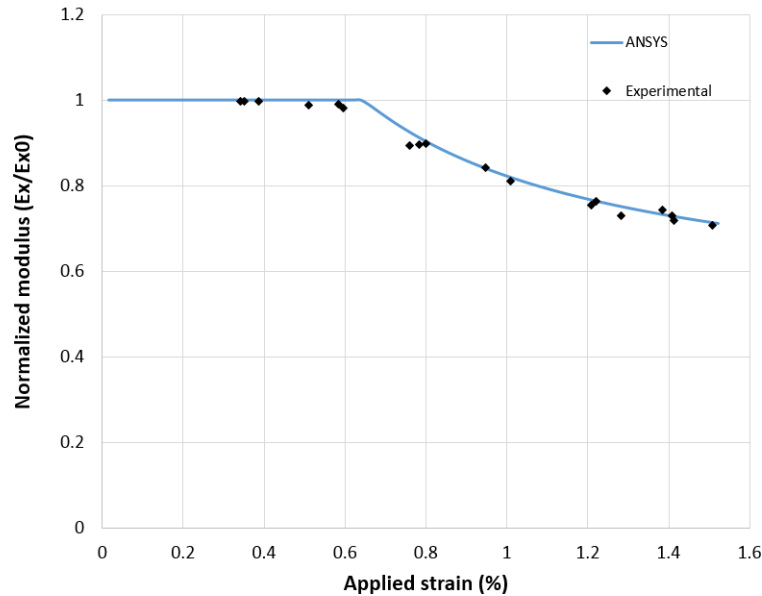


Figure 12: Normalized modulus vs. applied strain for laminate  $[\pm 15/90_4]_s$ .

Since  $G_c$  was adjusted with laminate #1, where cracks propagate under pure mode I (opening), damage evolution is predicted well as long as there is no contribution from mode II (shear). This can be seen in Figures 5, and 12 through 15, but not on Figures 16–18, because on angle-ply clusters, cracks propagate under mixed mode conditions.

PDA does not have a separate dissipation energy parameter to handle a second mode of crack propagation. While it is possible to adjust the single value of  $G_c$  with data combining more than one laminate (say #1 and #8), or from a laminate under mixed mode (say #8), the predictions for all the cross-ply laminates would suffer appreciably. Thus, such option was discarded in this study. In summary, the single value of dissipation energy  $G_c$  should be adjusted with laminates experiencing the mixed-mode conditions expected in practice. This is not always feasible, given the variety of laminates usually employed in design.

Also note that the value of  $F_6$  adjusted with laminate #8 does not accurately predict damage initiation for laminate #8 (Figure 17). This is because  $F_6$  is the only parameter remaining (after  $F_{2t}$  and  $G_c$  were adjusted with laminate #1) to minimize the error in Figure 17. Therefore, the optimization chooses a value that is too high but that minimizes the error. We could force the shear strength value to be adjusted with the damage onset only, but then the prediction of damage evolution of all the laminates with mixed-mode cracking would suffer appreciably. It would seem that PDA would benefit from having another parameter to account for mixed-mode cracking. Similarly, correction of in situ strength for cluster thickness would improve the prediction of damage initiation.

## 5. Mesh sensitivity

Mesh sensitivity refers to how much the solution changes with mesh density, number of elements, number of nodes, and element type used to discretize the problem under study. There are two sources of mesh sensitivity. The most obvious is type I sensitivity, where the quality of the solution, particularly stress and

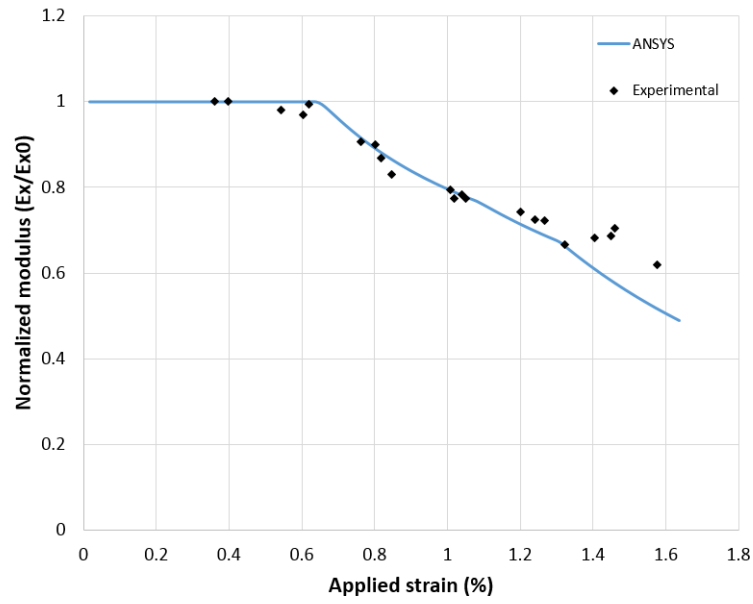


Figure 13: Normalized modulus vs. applied strain for laminate  $[\pm 30/90_4]_s$ .

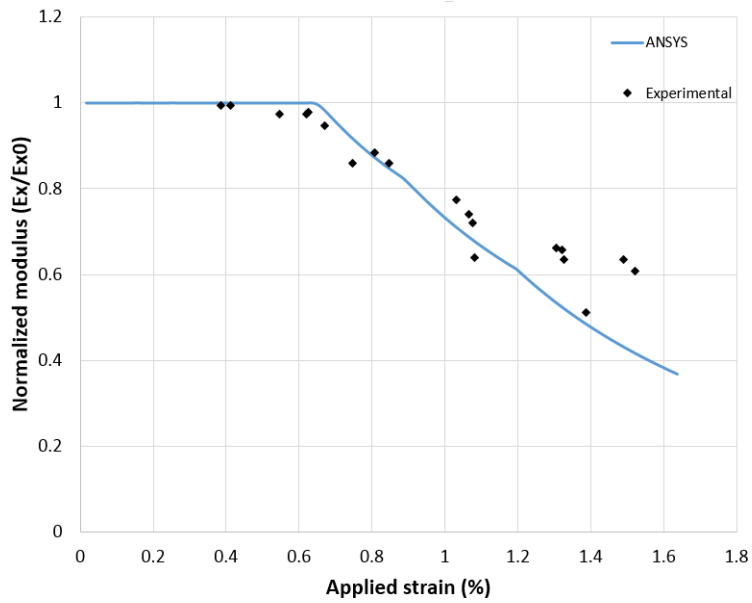


Figure 14: Normalized modulus vs. applied strain for laminate  $[\pm 40/90_4]_s$ .

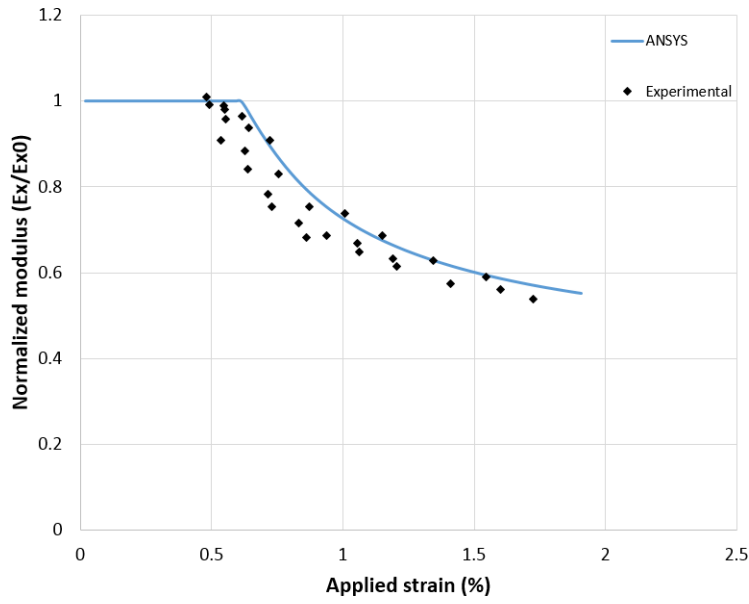


Figure 15: Normalized modulus vs. applied strain for laminate  $[0/90_8/0_{0.5}]_s$ .

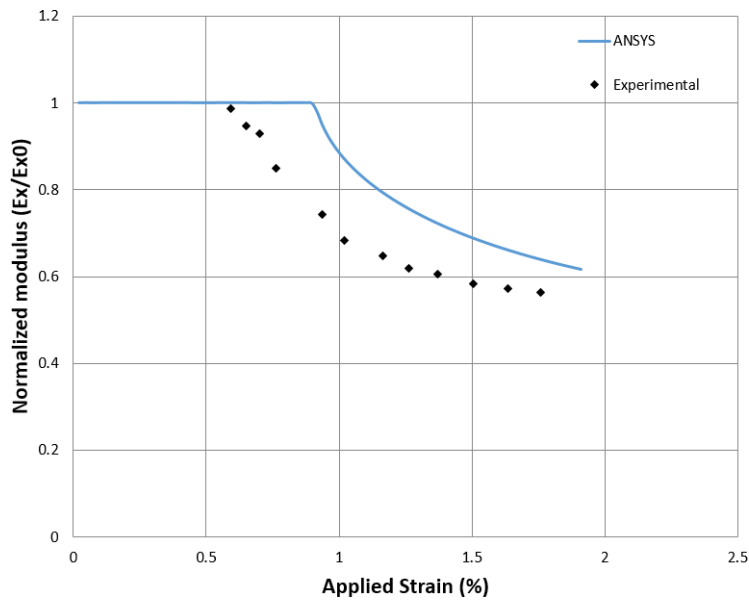


Figure 16: Normalized modulus vs. applied strain for laminate  $[0/\pm 70_4/0_{0.5}]_s$ .

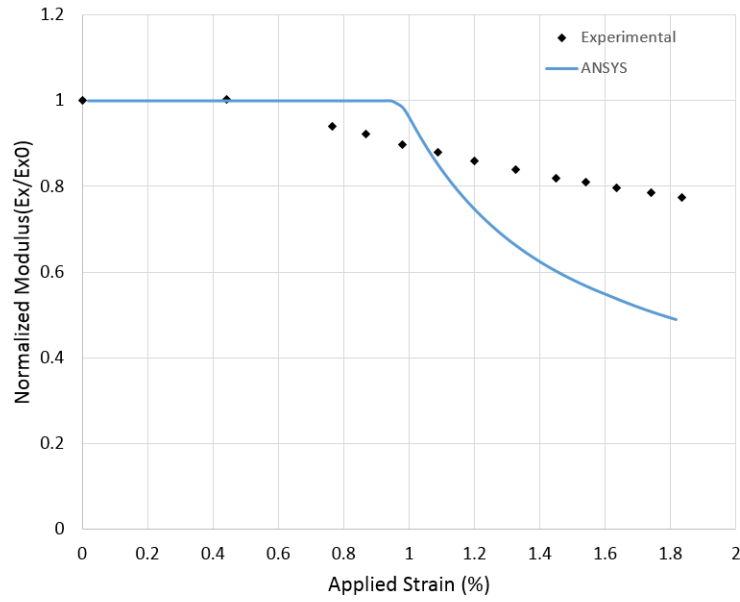


Figure 17: Normalized modulus vs. applied strain for laminate  $[0/\pm 40_4/0_{0.5}]_s$ .

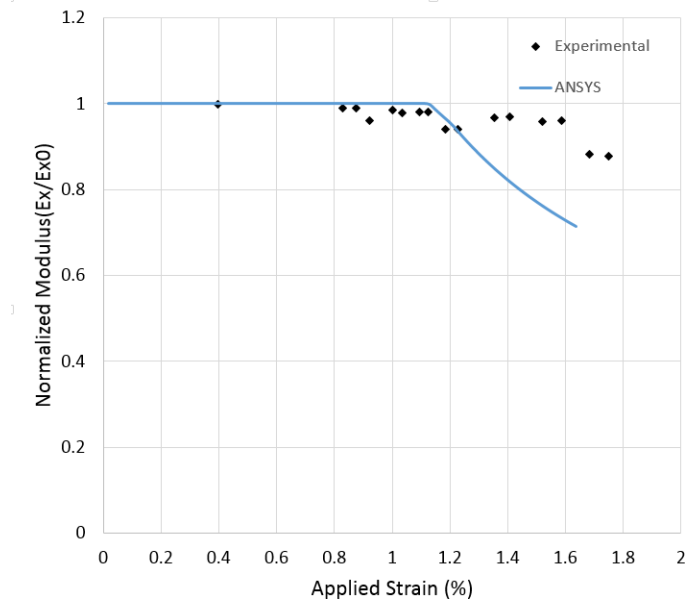


Figure 18: Normalized modulus vs. applied strain for laminate  $[0/\pm 25_4/0_{0.5}]_s$ .

strain gradients, depends on mesh density; the finer the mesh, the better the accuracy of the solution. Assuming that the mesh is refined enough to capture stress/strain gradients satisfactorily, type II sensitivity may come from the constitutive model used.

When the material response is non-linear, the constitutive model calculates the stress for a given strain and updates one or more state variables to keep track of the history of the material state. Ideally, the response of the constitutive model should be independent of the mesh.

To isolate the two sources of mesh dependency, it is customary to test the software with examples for which the strain field is uniform in the domain regardless of mesh density. The physical tensile test in this study experiences uniform strain everywhere in the rectangular domain representing the gage section of the specimen. Under these conditions, there is no type I mesh sensitivity in the calculation of displacement and strain because the strain is uniform for the experimental conditions used (ASTM D 3039). However, the reaction force still depends on the accuracy of the constitutive model.

It is customary in the FEM literature [5, 39, 40, 41, 42, 43] to assess mesh sensitivity using force-displacement or force-strain plots. Stress-strain is not used because stress is calculated by the constitutive model, which is the potential source of mesh sensitivity being investigated. The definite proof is provided by force equilibrium, thus force must be reported. Since we do not have access to the actual code implementation, we are unable to pinpoint the source of mesh dependency but we are only able to report that mesh dependency was observed in the results for the examples that we considered in this study. For a more thorough explanation of this issue, the reader may wish to consult [39].

It can be seen in Fig. 19 that ANSYS/PDA is sensitive to h-refinement (mesh refinement), displaying softer behavior when the mesh is refined. However, ANSYS/PDA is not sensitive to p-refinement (using higher order elements). In fact, the material parameters in this study were obtained with SHELL 181, which is a linear element (4 nodes), but the predictions are unaffected by switching to SHELL 281, which is a quadratic element (8 nodes).

## 6. Conclusions

A novel methodology is proposed to determine the material parameters for Progressive Damage Analysis (PDA) in ANSYS and the procedure is explained in detail.

It is observed that adjusted material parameters  $F_{2t}$ ,  $F_6$ ,  $G_c$ , can be used to predict damage initiation and evolution in laminated composites using ANSYS, and that good comparison with available experimental data can be achieved with certain restrictions.

The in situ strength values  $F_{2t}$  and  $F_6$  should be adjusted with data from laminates with similar cluster thickness to those expected in practice. The single value of dissipation energy  $G_c$  should be adjusted with laminates experiencing similar mixed-mode fracture conditions to those expected in practice. This is not always feasible, given the variety of laminates usually employed in design. A second dissipation energy parameter, besides  $G_c$ , could be added to the PDA formulation to improve the predictions when the mixed-mode fracture conditions vary. Similarly, an algorithm to correct the strength values for in situ effect as a function of ply-cluster thicknesses could be added to PDA to improve the prediction of damage onset.

The damage parameters of PDA can be calculated from measured laminate stiffness degradation but they are not directly measurable parameters, as it is, for example, the crack density. PDA can predict reduction of stiffness, and uses damage parameters to do so, but it cannot predict crack density.

ANSYS/PDA predictions are shown to be dependent of mesh density, number of elements, and number of nodes, but independent of element type.

When compared to direct optimization methods, response surface demonstrates two advantages. First, it allows for fast computation of the sensitivity of the error to the material parameters sought, thus allowing the



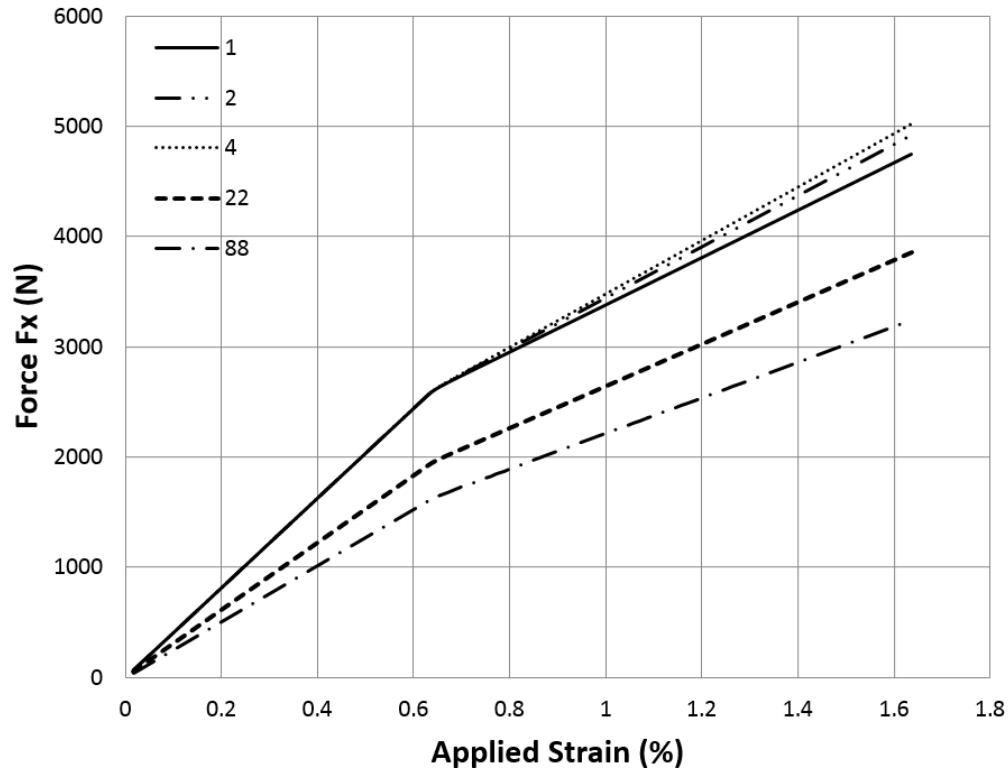


Figure 19: Force vs. applied strain for laminate  $[0_2/90_4]_s$  using different number of elements.

analyst to select the most appropriate laminate stacking sequence to adjust each material property. Second, RS is able to adjust the material parameters accurately and with low computational expense. However, the direct optimization method is always available to perform a final check.

### Acknowledgments

The authors acknowledge the infrastructure support from the Energy Materials Science and Engineering (EMSE) program at West Virginia University.

### Bibliography

- [1] M. V. Donadon, S. F. M. D. Almeida, M. A. Arbelo, A. R. de Faria, A three-dimensional ply failure model for composite structures, *International Journal of Aerospace Engineering (Hindawi)* 2009 (486063).
- [2] P. Ladevèze, O. Allix, J. F. Deü, D. Lévêque, A mesomodel for localisation and damage computation in laminates, in: *Computer Methods in Applied Mechanics and Engineering*, Vol. 183, 2000, pp. 105–122.

- [3] E. Abisset, F. Daghia, P. Ladevèze, On the validation of a damage mesomodel for laminated composites by means of open-hole tensile tests on quasi-isotropic laminates, *Composites Part A* 42 (10) (2011) 1515–1524.
- [4] F. Rastellini, S. Oller, O. S. E. Onate, Composite materials non-linear modelling for long fibre-reinforced laminates continuum basis computational aspects and validations, *Computers & Structures* 86 (9) (2008) 879–896.
- [5] X. Martinez, S. Oller, Numerical simulation of matrix reinforced composite materials subjected to compression loads, *Archives of computational methods in engineering* 16 (4) (2009) 357–397.
- [6] X. Martinez, F. Rastellini, S. Oller, F. Flores, E. Onate, Computationally optimized formulation for the simulation of composite materials and delamination failures, *Composites Part B* 42 (2) (2011) 134–144.
- [7] Firehole Composites, Helius MCT Composite Materials Analysis Software, 2016, <http://www.firehole.com/products/mct/>.
- [8] E. Barbero, P. Lonetti, Damage model for composites defined in terms of available data, *Mechanics of Composite Materials and Structures* 8 (4) (2001) 299–315.
- [9] A. Matzenmiller, J. Lubliner, R. Taylor, A constitutive model for anisotropic damage in fiber-composites, *Mechanics of Materials* 20 (1995) 125–152.
- [10] P. Camanho, C. Davila, Mixed-mode decohesion finite elements for the simulation of delamination in composite materials, in: NASA TM 2002–211737, 2002, pp. 1–37.
- [11] D. H. Cortes, E. J. Barbero, Stiffness reduction and fracture evolution of oblique matrix cracks in composite laminates, *Annals of Solid and Structural Mechanics* 1 (1) (2010) 29–40.
- [12] R. J. Nuismer, S. C. Tan, Constitutive relations of a cracked composite lamina, *Journal of Composite Materials* 22 (306) (1988) 306–321.
- [13] S. C. Tan, R. J. Nuismer, A theory for progressive matrix cracking in composite laminates, *Journal of Composite Materials* 23 (1989) 1029–1047.
- [14] E. Adolfsson, P. Gudmundson, Matrix crack initiation and progression in composite laminates subjected to bending and extension, *International Journal of Solids and Structures* 36 (1999) 3131–3169.
- [15] J. M. Berthelot, Transverse cracking and delamination in cross-ply glass-fiber and carbon-fiber reinforced plastic laminates: static and fatigue loading, *Applied Mechanics Review* 56 (2003) 111–147.
- [16] A. Adumitroaie, E. J. Barbero, Intralaminar damage model for laminates subjected to membrane and flexural deformations, *Mechanics of Advanced Materials and Structures* 22 (9) (2015) 705–716. doi:10.1080/15376494.2013.796541.
- [17] J. A. Nairn, *Finite Fracture Mechanics of Matrix Microcracking in Composites. Application of Fracture Mechanics to Polymers, Adhesives and Composites*, Elsevier, 2004.
- [18] S. H. Lim, S. Li, Energy release rates for transverse cracking and delaminations induced by transverse cracks in laminated composites, *Composites Part A* 36 (11) (2005) 1467–1476.

- [19] D. T. G. Katerelos, M. Kashtalyan, C. Soutis, C. Galiotis, Matrix cracking in polymeric composites laminates: Modeling and experiments, *Composites Science and Technology* 68 (2008) 2310–17.
- [20] D. T. G. Katerelos, J. Varna, C. Galiotis, Energy criterion for modeling damage evolution in cross-ply composite laminates, *Composites Science and Technology* 68 (2008) 2318–24.
- [21] J. Varna, R. Joffe, R. Talreja, A synergistic damage-mechanics analysis of transverse cracking [/904]s laminates, *Composites Science and Technology* 61 (5) (2001) 657–665.
- [22] G. Alfano, M. Crisfield, Finite element interface models for the delamination analysis of laminated composites: Mechanical and computational issues, *International Journal for Numerical Methods in Engineering* 50 (7) (2001) 1701–1736.
- [23] Alpha STAR Corporation, Genoa virtual testing & analysis software,, 2016, <http://www.ascgenoa.com>.
- [24] ANSYS, Mechanical APDL, Advanced Analysis Guide, 9. User-Programmable Features, SAS IP, Inc, 17th Edition (2016).
- [25] J. Varna, R. Joffe, N. Akshantala, R. Talreja, Damage in composite laminates with off-axis plies, *Composites Science and Technology* 59 (14) (1999) 2139–2147.
- [26] R. Talreja, S. Yalvac, L. Yats, D. Wetters, Transverse cracking and stiffness reduction in cross ply laminates of different matrix toughness, *Journal of Composite Materials* 26 (11) (1992) 1644–1663.
- [27] P. Camanho, C. Davila, S. Pinho, L. Iannucci, P. Robinson, Prediction of in situ strengths and matrix cracking in composites under transverse tension and in-plane shear, *Composites Part A: Applied Science and Manufacturing* 37 (2) (2006) 165–176.
- [28] Z. Hashin, A. Rotem, Fatigue failure criterion for fiber reinforced materials, *Journal of Composite Materials* 7 (1973) 448–464.
- [29] B. W. Rosen, Tensile failure of fibrous composites, *AIAA J* 2 (11) (1964) 1985–1991.
- [30] B. W. Rosen, *Fiber Composite Materials (Chapter 3)*, ASM International, Metals Park, OH, 1965.
- [31] E. J. Barbero, Prediction of compression strength of unidirectional polymer matrix composites, *Journal of Composite Materials* 32 (5) (1998) 483–502.
- [32] P. Camanho, C. Davila, S. Pinho, L. Iannucci, P. Robinson, Prediction of in situ strengths and matrix cracking in composites under transverse tension and in-plane shear, *Composites Part A: Applied Science and Manufacturing* 37 (2) (2006) 165–176.
- [33] E. J. Barbero, *Introduction to Composite Materials Design*, 2nd Edition, CRC Press, 2011.
- [34] C. Davila, P. Camanho, C. Rose, Failure criteria for FRP laminates, *Journal of Composite Materials* 39 (4) (2005) 323–345.
- [35] A. S. D. Wang, Fracture mechanics of sublaminar cracks in composite materials, *Compos. Tech. Review* 6 (1984) 45–62.
- [36] ANSYS, Mechanical APDL, Material Reference, 4. Nonlinear Material Properties, 4.24. Material Damage, SAS IP, Inc, 17th Edition (2016).

- [37] ANSYS, DesignXplorer User's Guide, SAS IP, Inc, 17th Edition (2016).
- [38] E. J. Barbero, Cadec-online.com Release 14, <http://cadec-online.com> (2016).
- [39] J. Oliver, A consistent characteristic length for smeared cracking models, *International Journal for Numerical Methods in Engineering* 28 (2) (1989) 461–474.
- [40] X. Martinez, S. Oller, L. Barbu, A. Barbat, A. De Jesus, Analysis of ultra low cycle fatigue problems with the barcelona plastic damage model and a new isotropic hardening law, *International Journal of Fatigue* 73 (2015) 132 – 142.
- [41] F. Otero, X. Martinez, S. Oller, O. Salomon, An efficient multi-scale method for non-linear analysis of composite structures, *Composite Structures* 131 (2015) 707 – 719.
- [42] Madeo, A., Casciaro, R., Zagari, G., Zinno, R., Zucco, G., A mixed isostatic 16 dof quadrilateral membrane element with drilling rotations based on Airy stresses, *Finite Elements in Analysis and Design* 89 (2014) 52 – 66.
- [43] Ungureanu, V. , Dubina, D., Crisan, , Madeo, A., Zagari, G., Zucco, G., Zinno, R., Koiter asymptotic analysis of thin-walled cold-formed steel members, *Acta Mechanica et Automatica* 9 (2015) 245 – 251.